

# Measurement of Differences Between $J/\psi$ and $\psi'$ Suppression in p-A Collisions

M.J. Leitch<sup>f</sup>, W.M. Lee<sup>d</sup>, M.E. Beddo<sup>g</sup>, C.N. Brown<sup>e</sup>, T.A. Carey<sup>f</sup>, T.H. Chang<sup>g\*</sup>, W.E. Cooper<sup>c</sup>, C.A. Gagliardi<sup>i</sup>, G.T. Garvey<sup>f</sup>, D.F. Geesaman<sup>b</sup>, E.A. Hawker<sup>i,f</sup>, X.C. He<sup>d</sup>, L.D. Isenhower<sup>a</sup>, D.M. Kaplan<sup>e</sup>, S.B. Kaufman<sup>b</sup>, D.D. Koetke<sup>j</sup>, P.L. McGaughey<sup>f</sup>, J.M. Moss<sup>f</sup>, B.A. Mueller<sup>b</sup>, V. Papavassiliou<sup>g</sup>, J.C. Peng<sup>f</sup>, G. Petitt<sup>d</sup>, P.E. Reimer<sup>f,b</sup>, M.E. Sadler<sup>a</sup>, W.E. Sondheim<sup>f</sup>, P.W. Stankus<sup>h</sup>, R.S. Towell<sup>a,f</sup>, R.E. Tribble<sup>i</sup>, M.A. Vasiliev<sup>i,†</sup>, J.C. Webb<sup>g</sup>, J.L. Willis<sup>a</sup>, G.R. Young<sup>h</sup>

(FNAL E866/NuSea Collaboration)

<sup>a</sup>Abilene Christian University, Abilene, TX 79699

<sup>b</sup>Argonne National Laboratory, Argonne, IL 60439

<sup>c</sup>Fermi National Accelerator Laboratory, Batavia, IL 60510

<sup>d</sup>Georgia State University, Atlanta, GA 30303

<sup>e</sup>Illinois Institute of Technology, Chicago, IL 60616

<sup>f</sup>Los Alamos National Laboratory, Los Alamos, NM 87545

<sup>g</sup>New Mexico State University, Las Cruces, NM, 88003

<sup>h</sup>Oak Ridge National Laboratory, Oak Ridge, TN 37831

<sup>i</sup>Texas A & M University, College Station, TX 77843

<sup>j</sup>Valparaiso University, Valparaiso, IN 46383

(December 15, 2005)

Measurements of the suppression of the yield per nucleon of  $J/\psi$  and  $\psi'$  production for 800 GeV/c protons incident on heavy relative to light nuclear targets have been made with very broad coverage in  $x_F$  and  $p_T$ . The observed suppression is smallest at  $x_F$  values of 0.25 and below and increases at larger values of  $x_F$ . It is also strongest at small  $p_T$ . Substantial differences between the  $\psi'$  and  $J/\psi$  are observed for the first time in p-A collisions. The suppression for the  $\psi'$  is stronger than that for the  $J/\psi$  for  $x_F$  near zero, but becomes comparable to that for the  $J/\psi$  for  $x_F > 0.6$ .

24.85.+p; 13.85.Qk; 14.40.Lb; 14.65.Dw

Strong suppression of the yield per nucleon of heavy vector mesons produced in heavy nuclei relative to that in light nuclei has been observed in proton and pion-nucleus collisions [1–6]. Similar effects have also been observed in heavy-ion collisions [7]. This suppression exhibits strong kinematic dependences, especially with Feynman- $x$  ( $x_F$ ) and transverse momentum ( $p_T$ ) of the produced vector meson. Since the suppression of heavy vector meson production in heavy-ion collisions is predicted to be an important signature for the formation of the quark-gluon plasma (QGP), it is important to understand the mechanisms that can produce similar effects in the absence of a QGP. These mechanisms can be studied in proton-nucleus production of vector mesons where no QGP is presumed to occur. Many effects have been considered [8–11] in attempting to describe the observed proton-induced charmonium yields from nuclear targets, e.g. absorption, parton energy loss, shadowing and feed-down from higher mass resonances, but it is clear that no adequate understanding of the problem has been achieved. Even the absolute cross sections are poorly understood due to poor knowledge of the production mechanism, and most models ignore or use naive pictures of the space-time evolution of the  $c\bar{c}$  pair. Recognizing that the production and suppression mechanisms can be identified by their strong kinematic dependences, it is

crucial to have new data with broad kinematic coverage to challenge comprehensive descriptions of charmonium production in nuclei.

Here we report new high statistics measurements made in Fermilab E866/NuSea of the nuclear dependence of  $J/\psi$  and  $\psi'$  production for proton-nucleus collisions on Be, Fe, and W targets. Over  $3 \times 10^6$   $J/\psi$ 's and  $10^5$   $\psi'$ 's with  $x_F$  between  $-0.10$  and  $0.93$  and  $p_T$  up to  $4$  GeV/c were observed. Previous measurements in E772 [1] and E789 [3,2] have suffered from limited  $p_T$  acceptance and limited statistics at larger values of  $x_F$ , both of which are greatly extended in these new data.

E866/NuSea used a 3-dipole magnet pair spectrometer employed in previous experiments (E605 [12], E772, and E789), modified by the addition of new drift chambers and hodoscopes with larger acceptance at the first tracking station and a new trigger system [13]. This spectrometer was also used for other measurements in E866/NuSea [14,15]. An 800 GeV/c extracted proton beam of up to  $6 \times 10^{11}$  protons per 20 s spill bombarded the targets used in these measurements. A rotating wheel which was located upstream of either the first or second magnet held thin solid targets of Be, Fe and W with thicknesses corresponding to between 3% and 19% of an interaction length. After passing through the target, the remaining beam was absorbed in a copper beam dump

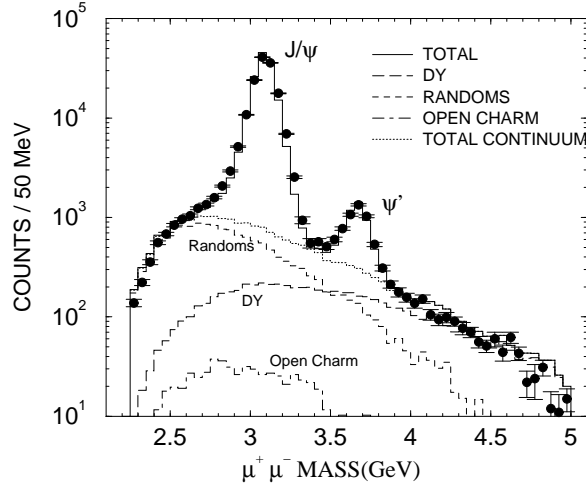


FIG. 1. Fit to the mass spectrum for the Be target in the  $x_F$  range from 0.00 to 0.05. Components in the fit are the  $J/\psi$ , the  $\psi'$ , Drell-Yan (long-dashed), randoms (short-dashed), and open charm (dot-dash). The solid curve represents the total of all fitted lineshapes and the dotted curve represents the continuum which is the sum of the Drell-Yan, randoms and open charm.

located inside the large second magnet. Following the beam dump was a 13.4 interaction length absorber wall which filled the entire aperture of the magnet, eliminated hadrons, and assured that only muons traversed the spectrometer's detectors. These muons were then tracked through a series of detector stations composed of drift chambers, hodoscopes and proportional tubes. Because of improvements in the trigger system, the coverage in  $p_T$  was much broader than in previous experiments with this spectrometer (e.g. E772), extending to over 4 GeV/c. Beam intensity was monitored using secondary-emission detectors.

Three magnetic field and target location configurations were used to span the full range in  $x_F$ : small- $x_F$  (SXF,  $-0.1 \leq x_F \leq 0.3$ ), intermediate- $x_F$  (IXF,  $0.2 \leq x_F \leq 0.6$ ) and large- $x_F$  (LXF,  $0.3 \leq x_F \leq 0.93$ ). Detailed Monte Carlo simulations of the  $J/\psi$  and  $\psi'$  peaks and of the Drell-Yan continuum were used to generate lineshapes in each bin in  $x_F$  or in  $p_T$ . For the Drell-Yan calculations we use MRST [16] NLO with EKS98 [17] shadowing corrections. The contribution to the continuum from semi-leptonic decay to muons of open charm pairs was estimated using PYTHIA [18] and a small correction, less than half the statistical uncertainties, was made for it in the SXF data set; but for the larger  $x_F$  data sets it is negligible and no corrections were made. In addition, a detailed construction of random muon pairs using single-muon events (which also provided a good fit to the like-sign muon mass spectra) was used to account for the smooth random background underneath the peaks. A maximum-likelihood method was used for fitting that took into account the statistical uncertainty of the data

and of the Monte Carlo and randoms [19]. Figure 1 shows a typical fit to a mass spectrum using these components. Since the rates in the various detectors were nearly equal for the different targets, a correction for rate-dependent inefficiencies was not necessary.

We present our results in terms of  $\alpha$ , where  $\alpha$  is obtained by assuming the cross section dependence on nuclear mass,  $A$ , to be of the form  $\sigma_A = \sigma_N \times A^\alpha$ , where  $\sigma_N$  is the cross section on a nucleon. For the SXF data,  $\alpha$  was obtained using Be and two different thickness  $W$  targets, while for the IXF and LXF data, Be, Fe and  $W$  targets were used. The SXF data from the two  $W$  targets verified that no corrections for secondary production were necessary. The  $p_T$  dependence of  $\alpha$  is shown in Fig. 2, where we see essentially the same increase in  $\alpha$  for all  $x_F$  ranges for both the  $J/\psi$  and the  $\psi'$ , as well as for the 200 GeV/c NA3 data [4]. This increase is characteristic of multiple scattering of the incident parton and of the nascent  $c\bar{c}$  in the final state. Note that for the IXF data the  $p_T$  acceptance is truncated at about 2 GeV/c because a more restrictive trigger was used.

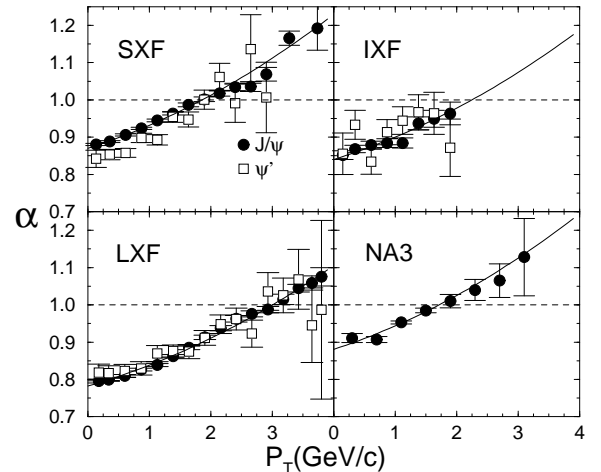


FIG. 2.  $\alpha$  versus  $p_T$  for  $J/\psi$  (solid circles) and  $\psi'$  (open boxes) production by 800 GeV/c protons. Results are shown for the three data sets – SXF, IXF and LXF (see text) – which have  $\langle x_F \rangle = 0.055, 0.308$  and  $0.480$ , respectively. Only statistical uncertainties are shown. An additional systematic uncertainty of 0.5% is not included. Also shown are the NA3 results at 200 GeV/c whose  $x_F$  range can be seen in Fig. 4. The solid curves represent the parameterization discussed in the text.

Previous experiments such as E772 have had a limited acceptance in  $p_T$  which varied with  $x_F$ . Since the value of  $\alpha$  depends strongly on  $p_T$  this can cause a distortion of the apparent shape of  $\alpha$  versus  $x_F$ . The improvements in the E866/NuSea trigger allowed a much broader  $p_T$  acceptance than in these earlier measurements. However, for the lowest values of  $x_F$  at each spectrometer setting our  $p_T$  acceptance still becomes somewhat restricted. For the results presented here we have corrected the values of  $\alpha(x_F)$  using a detailed simulation of our acceptance and

a differential cross section shape versus  $p_T$  derived from our data.

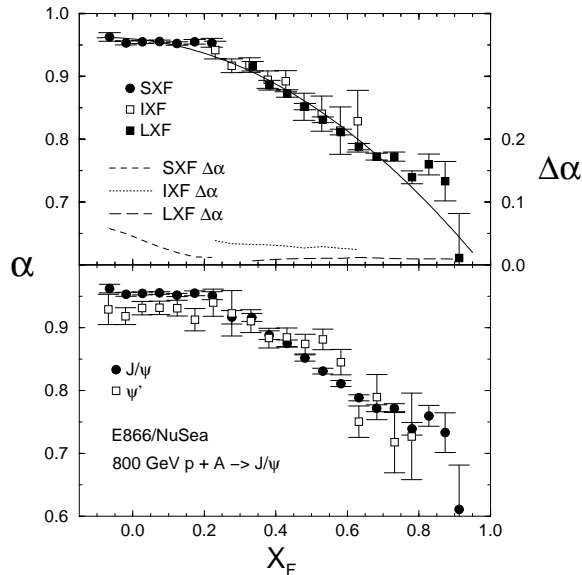


FIG. 3.  $\alpha$  for the  $J/\psi$  versus  $x_F$  for the three different data sets (top) and for the  $J/\psi$  and  $\psi'$  after the data sets are combined (bottom). Values are corrected for the  $p_T$  acceptance, as discussed in the text. These corrections ( $\Delta\alpha$ ) have a maximum value of 0.06 and are shown using the right-hand vertical scale in the top panel. The relative systematic uncertainty between  $\alpha$  for the  $J/\psi$  and  $\psi'$  is estimated to be 0.003, while the absolute systematic uncertainty is 0.01 in  $\alpha$ ; neither is included here. The solid curve represents the parameterization discussed in the text.

The resulting dependence of  $\alpha$  on  $x_F$  is shown in Fig. 3 and listed in Table I. The systematic uncertainty of 1% in the corrected  $\alpha$  is dominated by the  $p_T$  acceptance correction.  $\alpha$  for the  $J/\psi$  is largest at values of  $x_F$  of 0.25 and below but strongly decreases at larger values of  $x_F$ . For the  $\psi'$   $\alpha$  is smaller than for the  $J/\psi$  for  $x_F < 0.2$ , remains relatively constant up to  $x_F$  of 0.5 (becoming slightly larger than for the  $J/\psi$ ) and then falls to values consistent with those for the  $J/\psi$  for  $x_F > 0.6$ . The significance of the overall  $J/\psi$ ,  $\psi'$  difference for  $x_F < 0.2$  is about 4 sigma with respect to the statistical and relative systematic uncertainties. This difference is consistent with less accurate results obtained by NA38 for p-A at 450 GeV/c [6], but is inconsistent with the quoted NA38 result that also included the p-p and p-d data from NA51. Although slightly larger  $\alpha$  values for the  $\psi'$  than for the  $J/\psi$  can be seen near  $x_F = 0.55$ , we should point out that if instead we emphasize the velocity of the  $c\bar{c}$  and plot  $\alpha$  versus rapidity, then the agreement is quite good in this region. The reduced  $\alpha$  at small  $x_F$  is also evident in Fig. 2 where  $\alpha$  for the  $\psi'$  falls consistently below that for the  $J/\psi$  at low  $p_T$  for the SXF data set.

Our results for the  $J/\psi$   $\alpha$  can be represented for convenience by the simple parameterizations shown as solid lines in Figs. 2 and 3:  $\alpha(x_F) = 0.960(1 - 0.0519x_F -$

TABLE I.  $\alpha$  versus  $x_F$  [20] for the  $J/\psi$  and  $\psi'$ .  $\alpha$  is defined by  $\sigma_A = \sigma_N \times A^\alpha$  and is equal to one if there is no suppression and the cross section scales simply as the number of nucleons. The average momentum fraction of the struck parton,  $x_2$  [21], and the center-of-mass rapidity,  $y_{cm}$ , are also shown. An additional systematic uncertainty of 1% is not included here.

$\langle x_F \rangle$	$\langle y_{cm} \rangle_{J/\psi}$	$\langle x_2 \rangle_{J/\psi}$	$\alpha_{J/\psi}$	$\langle y_{cm} \rangle_{\psi'}$	$\langle x_2 \rangle_{\psi'}$	$\alpha_{\psi'}$
-0.065	-0.390	0.1192	0.962(7)	-0.344	0.1346	0.929(24)
-0.019	-0.115	0.0902	0.953(3)	-0.104	0.1056	0.918(14)
0.027	0.161	0.0679	0.955(2)	0.132	0.0828	0.931(11)
0.075	0.433	0.0511	0.955(2)	0.369	0.0645	0.932(11)
0.124	0.680	0.0395	0.952(3)	0.588	0.0513	0.931(12)
0.173	0.896	0.0316	0.955(4)	0.785	0.0418	0.913(18)
0.223	1.091	0.0262	0.951(6)	0.974	0.0347	0.940(22)
0.277	1.288	0.0213	0.917(11)	1.144	0.0293	0.923(36)
0.332	1.427	0.0182	0.916(6)	1.281	0.0253	0.910(18)
0.381	1.551	0.0160	0.888(7)	1.401	0.0223	0.884(16)
0.431	1.663	0.0142	0.875(6)	1.512	0.0199	0.885(15)
0.481	1.764	0.0128	0.852(5)	1.614	0.0179	0.874(16)
0.531	1.858	0.0117	0.831(5)	1.705	0.0163	0.881(16)
0.582	1.945	0.0107	0.811(5)	1.791	0.0150	0.845(20)
0.632	2.026	0.00984	0.789(6)	1.869	0.0138	0.751(25)
0.682	2.098	0.00916	0.772(5)	1.942	0.0129	0.790(36)
0.732	2.166	0.00855	0.772(7)	2.009	0.0120	0.718(49)
0.781	2.228	0.00804	0.739(10)	2.071	0.0113	0.727(69)
0.828	2.286	0.00760	0.760(17)			
0.873	2.338	0.00723	0.733(32)			
0.913	2.383	0.00698	0.611(71)			

$0.338x_F^2$ ), and  $\alpha(p_T) = A_i(1 + 0.0604p_T + 0.0107p_T^2)$ , where  $A_i = 0.870, 0.840, 0.782$  and  $0.881$  for the SXF, IXF and LXF datasets and for the NA3 data, respectively.

A comparison of our results with earlier data from E772 at 800 GeV/c [1] and also with NA3 at 200 GeV/c [4] is shown in Fig. 4. It illustrates that the suppression seen for  $J/\psi$  production scales with  $x_F$  but not with  $p_{J/\psi}^{LAB}$  above about 90 GeV/c, which corresponds to  $x_F > 0.05$  for our data and to  $x_F > 0.4$  for NA3. Also of interest in these figures is a comparison of our results with those of E772. At the small- $x_F$  end of the E772 data their published results drop significantly below our results. As was discussed above, the E772 data have severe narrowing of the  $p_T$  acceptance for their smallest  $x_F$  bins, and a large correction that could easily bring the E772 points into agreement with our data is expected. Similar arguments hold for the E789  $J/\psi$  data (not shown) at small to negative  $x_F$  [3], where we estimate about an 8% correction which would bring those results into agreement with ours. On the other hand, the large  $x_F$  results from E789 [2] appear to be high by more than their systematic uncertainty of 2.5%.

The suppression of  $J/\psi$  production near  $x_F = 0$  is usually thought to be caused by absorption, the dissociation of the  $c\bar{c}$  pair by interactions with the nucleus or comovers [8] into separate quarks that eventually hadronize into  $D$  mesons. This model is supported by both the increased suppression of the  $\psi'$  that we observe near  $x_F = 0$  and

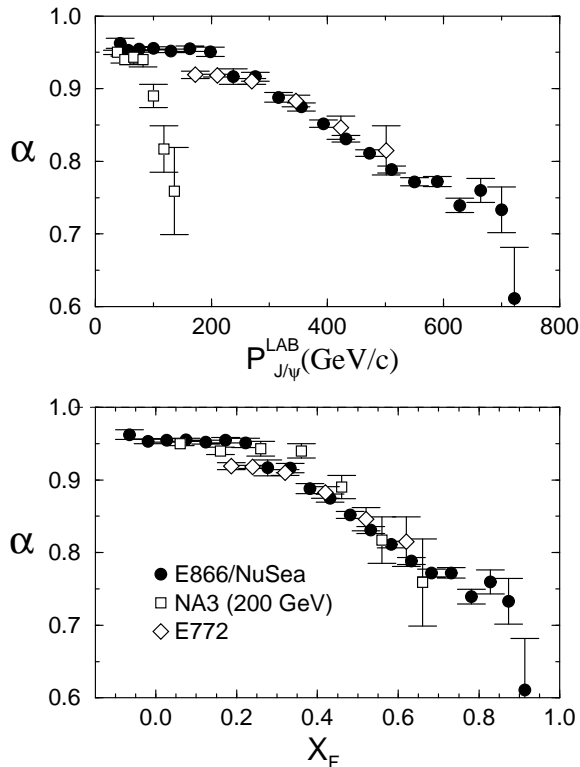


FIG. 4.  $\alpha$  versus  $x_F$  and versus  $p_{J/\psi}^{LAB}$  for the  $J/\psi$  from E866/NuSea (800 GeV/c) (solid circles) compared to E772 (open diamonds) and NA3 (200 GeV/c) (open squares) showing the scaling with  $x_F$  (bottom) and lack of scaling with  $p_{J/\psi}^{LAB}$  (top).

the absence of suppression of  $D$  meson production in the same kinematic region [22]. At small  $x_F$ , the velocity of the  $c\bar{c}$  pair is low enough that it may hadronize within the nucleus, so the larger  $\psi'$  would be absorbed more strongly [9,10]. However, the observed constancy of  $\alpha$  for both the  $J/\psi$  and the  $\psi'$  up to  $y_{cm} \simeq 1$  complicates this interpretation since these models predict that faster  $c\bar{c}$  pairs above  $x_F \simeq 0.1$  would experience similar absorption, whether they eventually hadronize outside the nucleus into a  $J/\psi$  or a  $\psi'$ . At larger values of  $x_F$ , above 0.3, our data does show similar suppression for the  $J/\psi$  and  $\psi'$ . Furthermore, if absorption by the nuclear medium is the dominant suppression mechanism, the effect should scale with  $p_{J/\psi}^{LAB}$ , but Fig. 4 shows that scaling breaks down in the middle of the region where we observe  $\alpha$  to be constant.

Shadowing of the small- $x$  target gluon distributions is also thought to play a role in the observed suppression, but current estimates [8,17] predict at most a few percent drop in  $\alpha(x_F)$ , even at the largest  $x_F$  values. Also, as is seen for our data (but not shown) and was seen previously [1], there is a lack of scaling with  $x_2$ , which is related to that shown above for  $p_{J/\psi}^{LAB}$  since  $x_2 \propto 1/p_{J/\psi}^{LAB}$ . This appears to rule out large contributions from shadowing. Our studies [14] show that for Drell-Yan the dominant

nuclear effect is shadowing of the anti-quark distributions and that the energy-loss of the incident quark is small. Although the incoming gluon's energy loss is expected to be larger by a color factor of 9/4 and the additional energy loss of the outgoing  $c\bar{c}$  may be as large as that of a gluon, we still expect the overall contribution of energy loss to be small for resonance production.

In conclusion, we have presented new data for the suppression of  $J/\psi$  and  $\psi'$  production in heavy versus light nuclei for 800 GeV/c proton-nucleus collisions. The kinematic coverage in  $x_F$  (-0.10 to 0.93) and  $p_T$  (0 - 4 GeV/c) and statistical accuracy surpass that of previous experiments. Corrections are made to the data to account for the narrowing  $p_T$  acceptance at the smaller values of  $x_F$ . The largest value of  $\alpha$  (integrated over  $p_T$ ) of about 0.95 is seen at  $x_F$  near 0.25 and below with strongly falling values for larger  $x_F$ . The most striking new result is that the suppression for the  $\psi'$  is stronger than that for the  $J/\psi$  at  $x_F$  near zero.

We thank Ramona Vogt and Boris Kopeliovich for many useful discussions and the Fermilab Particle Physics, Beams and Computing Divisions for their assistance. This work was supported in part by the U.S. Department of Energy.

\* Present address: University of Illinois, Urbana, IL 61801.

† On leave from Kurchatov Institute, Moscow, Russia.

- [1] D.M. Alde *et al.*, Phys. Rev. Lett. **66**, 133 (1991) and **66**, 2285 (1991).
- [2] M.S. Kowitt *et al.*, Phys. Rev. Lett. **72**, 1318 (1994).
- [3] M.J. Leitch *et al.*, Phys. Rev. **D52**, 4251 (1995).
- [4] J. Badier *et al.*, Z. Phys. **C20**, 101 (1983).
- [5] M.J. Corden *et al.*, Phys. Lett. B **110**, 415 (1982).
- [6] M.C. Abreu *et al.* Phys. Lett. B **444**, 516 (1998).
- [7] M.C. Abreu *et al.* Phys. Lett. B **450**, 456 (1999).
- [8] R. Vogt, hep-ph/9907317, and R. Vogt, S.J. Brodsky and P. Hoyer, Nucl. Phys. **B360**, 67 (1991).
- [9] F. Arleo, P.-B. Gossiaux, T. Gousset and J. Aichelin, hep-ph/9907286.
- [10] L. Gerland, L. Frankfurt, M. Strikman, H. Stöcker and W. Greiner, nucl-th/9908052.
- [11] Y.B. He, J. Hüfner and B.Z. Kopeliovich, hep-ph/9908243.
- [12] J.A. Crittenden *et al.*, Phys. Rev. **D34**, 2584 (1986).
- [13] C.A. Gagliardi *et al.*, Nucl. Instrum. Methods **A418**, 322 (1998).
- [14] M.A. Vasiliev *et al.* Phys. Rev. Lett. **83**, 2304 (1999).
- [15] E.A. Hawker *et al.*, Phys. Rev. Lett. **80**, 3715 (1998).
- [16] A.D. Martin, R.G. Roberts, W.J. Stirling, and R.S.Thorne, Eur. Phys. J. **C4**, 463 (1998).
- [17] K.J. Eskola, V.J. Kolhinen and C.A. Salgado, Eur. Phys. J. **C9**, 61 (1999).
- [18] H.-U. Bengtsson and T. Sjöstrand, Comp. Phys. Comm. **46**, 43 (1987).
- [19] HMCMLL from CERNLIB, R. Barlow and C. Beeston, Comp. Phys. Comm. **77**, 219 (1993).
- [20] We calculate  $x_F = p_L^{CM}/(\sqrt{s}/2)$ , neglecting a small ( $1 - \tau \simeq 0.6\%$ ) correction for the  $J/\psi$  mass.

- [21] We calculate  $x_2$  by ignoring the soft gluon that accompanies the  $c\bar{c}$  pair in the final state in the same way one would calculate  $x_2$  for the leading-order Drell-Yan process.
- [22] M.J. Leitch *et al.*, Phys. Rev. Lett. **72**, 2542 (1994).